INSTITUTE OF PHYSICS PUBLISHING JOURNAL OF PHYSICS B: ATOMIC, MOLECULAR AND OPTICAL PHYSICS

J. Phys. B: At. Mol. Opt. Phys. **34** (2001) 3493–3499 PII: S0953-4075(01)20799-8

Absolute photoionization cross section measurements of Xe^+ ions in the 4d threshold energy region

Yoh Itoh[1], Akira Ito[2], Masashi Kitajima[3], Tetsuo Koizumi[2], Takao M Kojima[4], Hiroshi Sakai[2], Mutsumi Sano[5] and Naoki Watanabe[6]

[1] Physics Laboratory, Josai University, Saitama 350-0295, Japan
[2] Department of Physics, Rikkyo University, Tokyo 171-8501, Japan
[3] Department of Physics, Sophia University, Tokyo 102-8554, Japan
[4] The Institute of Physical and Chemical Research, Saitama 351-0198, Japan
[5] Japan Synchrotron Radiation Research Institute (JASRI), Hyogo 679-5198, Japan
[6] Institute of Low Temperature Science, Hokkaido University, Hokkaido 060-0819, Japan

E-mail: yitoh@josai.ac.jp

Received 5 January 2001, in final form 19 July 2001
Published 27 August 2001
Online at stacks.iop.org/JPhysB/34/3493

Abstract

Using the photon–ion merged-beam technique, we have measured the absolute photoionization cross sections for Xe^{2+} and Xe^{3+} formation from Xe^+ at selected energies between 80 and 140 eV, and utilized the absolute data to normalize our previously reported relative cross sections. The structure and energy dependence of the cross sections for Xe^+ deviate from those of neutral Xe; however, the maximum total cross section for Xe^+ is, within the experimental error, the same as for Xe.

1. Introduction

The influence of the removal of outer electrons on inner-shell photoexcitation or photoionization processes has been attracting interest during the past two decades. Lucatorto *et al* [1] measured the photoabsorption spectra of Ba, Ba^+ and Ba^{2+} in the 4d threshold energy region using the dual laser-produced plasma (DLP) technique. The photoionization spectrum of Ba in the 4d threshold region is characterized by a so-called giant resonance peak [2]. They showed that when the two 5s electrons are removed from the outer shell of Ba, a drastic change happens, and many discrete lines appear in the lower energy region of the broad giant resonance peak. Later, Koizumi *et al* [3] showed that such a change does not occur abruptly by removal of the two outer electrons; the alteration of the spectra takes place continuously with the variation of the charge state of the target.

Several investigations have been made to study the photoionization processes of free ions along isonuclear sequences. D'Arcy *et al* [4] studied the photoabsorption spectra of Sb^+, Sb^{2+}, Sb^{3+} and Sb^{4+} using the DLP method, and the photon–ion merged-beam technique

has frequently been applied to measure cross sections. Kjeldsen *et al* [5] made absolute measurements for I^+ and I^{2+} targets, Sano *et al* [6], Koizumi *et al* [7] and Watanabe *et al* [8] reported relative cross sections for Xe^+, Xe^{2+} and Xe^{3+}, and Bizau *et al* [9] extended their measurements from Xe^{4+} to Xe^{7+} targets in the 4d region.

The 4d photoionization of Xe atoms is also characterized by the giant resonance peak due to the 4d–ϵf transition, and some preceding discrete peaks which correspond to 4d–6p, 7p transitions [10]. When the charge state of the Xe ion is increased, Koizumi *et al* [7] showed that (i) strong 4d–5p transitions occur around 55 eV and (ii) the intensities of the preceding peaks increase. So far, it has been very seldom [11] that absolute photoionization cross sections have been determined. Therefore, it has been unclear whether the discrete transitions govern the photoionization processes of these ions in the 4d region.

We report the absolute partial and total photoionization cross sections of Xe^+ ions ($4d^{10}5s^25p^5\ ^2P_{3/2,1/2}$) measured at selected energies between 80 and 140 eV. The aim of this paper is to study the quantitative changes of the giant resonance peak due to the removal of outer 5p electrons. To do that, the absolute cross sections were used to establish an absolute scale for the relative cross sections reported by our group [6, 7].

During the preparation of this paper, we were informed that Andersen *et al* [12] had also measured the absolute photoionization cross sections of Xe^+ and Xe^{2+} ions. The two sets of cross sections agree with each other within the experimental errors.

2. Experimental

Details of the photon–ion merged-beam apparatus used were described by Koizumi *et al* [3] and Sano *et al* [6], so only a brief description is given here. It consists of an electron-impact ion source, a Wien filter as a mass selector, quadrupole deflector, interaction region, electrostatic charge analyser and ion detectors. The Xe^+ ions were produced by an electron impact of about 150 eV at single collision conditions. It is known that almost all the ions are produced in the ground electronic configuration, $5s^25p^5$. The fractional ratio of $Xe^+(^2P_{3/2})$ and $Xe^+(^2P_{1/2})$ is determined by the statistical ratio, 2:1. The primary-beam intensity was about 80 nA.

The experimental method to determine the absolute cross section is the same as applied by Lyon *et al* [13]. We used the following equation to determine the cross section, σ:

$$\sigma = \frac{Se^2v\eta\Delta x\Delta y F_{\mathrm{av}}}{IJL\Omega} \tag{1}$$

where S is the signal counting rate, I the ion current measured by the Faraday cup, J the photodiode current, e the charge of an electron, v the velocity of the incident ions, L the length of the interaction region, and η and Ω are the detection efficiencies of the photodiode and ion detector, respectively. F_{av} is the linear average of the two-dimensional form factor, $F(z)$, along the beam axis z describing the beam overlap.

To determine the form factor, we introduced three pairs of movable slit into the interaction region. Each set consists of two slits which can be moved independently vertically and horizontally. The width of the slits was both 0.3 mm. The form factor is defined as

$$F(z) = \frac{1}{\Delta x\Delta y}\frac{\iint i\,\mathrm{d}x\,\mathrm{d}y\iint j\,\mathrm{d}x\,\mathrm{d}y}{\iint ij\,\mathrm{d}x\,\mathrm{d}y} \approx \frac{\sum\sum i\sum\sum j}{\sum\sum ij} \tag{2}$$

where i and j are the current elements measured by these slits at (x, y), whereas Δx and Δy are the stepping distance of the slits, which was normally 0.3 mm. A typical value for $\Delta x\Delta y F_{\mathrm{av}}/L$ was about 2.5×10^{-3} cm. The form factor measurement was repeated when the experimental conditions were changed. It took about 1 h to measure the form factor at the three positions inside the interaction region.

We added an einzel lens between the collimator and the interaction region to obtain better focusing, and nearly 100% of the ions were transferred from the interaction region to the detector system. The absolute intensity of the photon beam was determined by measuring the photocurrent from the Si photodiode calibrated at NIST [14]. The accuracy of the detector efficiency is claimed to be ±8% in the 100 eV region. The primary ion-beam current and the photodiode current were both measured by calibrated electrometers.

The charge states of the product ions were determined by an electrostatic charge-state analyser. The single- and double-photoionization cross sections could be measured at the same time. The analysed ions were further accelerated by a voltage of −3.2 kV before hitting a metal plate, placed in front of the detector, producing secondary electrons. The ion detection was performed by counting these electrons by channel electron multipliers. In the present setting, the energies of the analysed ions were 9.2 keV for Xe^{2+} ions and 13.2 keV for Xe^{3+} ions. These energies are considered to be large enough to produce at least one electron when an ion hits the metal surface; the detection efficiency Ω is assumed to be 1 for both Xe^{2+} and Xe^{3+} ions in the present data analysis. The error due to this assumption is estimated to be less than 10%.

The absolute cross section measurements were repeated several times at selected energies. A typical counting rate for the Xe^{3+} signal was 4000 s^{-1}, and the signal-to-noise ratio was about 3 in the region of 100 eV. The overall systematic error is estimated to be less than ±20% and the statistical error (the standard deviation of the mean) is evaluated to be about ±5%. The statistical error for the single-photoionization cross section is estimated to be ±40%. This large error bar is mainly due to the lower counting rate for the Xe^{2+} signal being less than 10% of the Xe^{3+} signal, while the background remained at the same order of magnitude.

The measurements were performed at the 2.5 GeV storage ring of the KEK photon factory at an undulator beam line (BL-16B). Photons were monochromatized by a 24 m spherical grating monochromator [15], with the typical photon flux estimated to be about 10^{13} s^{-1}. The energy calibration of the photon beam was done by measuring the discrete structures of neutral Xe at around 65 and 135 eV. The accuracy of the energy scale in the present measurement is estimated to be better than ±0.05 eV.

3. Results and discussions

3.1. Total photoionization cross section

The sum of absolute single- and double-photoionization cross sections, which were determined individually, are shown in figure 1. Each point represents the averaged value of several measurements, and the numerical values are given in table 1. The error bars represent the sum of the systematic and statistical errors.

As the threshold energy for triple ionization of Xe^+ is estimated to be 100 eV from the electron-impact data [16], the summed cross sections below 100 eV can be considered as the total photoionization cross section, whereas above 100 eV Xe^{4+} may contribute to the total cross section.

In figure 1, the sum of the previously determined single- and double-photoionization cross sections [6, 7], and the total photoionization cross section for neutral Xe [10, 17] are shown for comparison. The relative cross section for the Xe^+ target is normalized to the absolute scale at 103.6 eV. The absolute photoionization cross section for the Xe^+ ion is seen to be about 15% smaller than for neutral Xe at the giant resonance peak. The error bar of the cross section for neutral Xe is reported to be 2–3% [17].

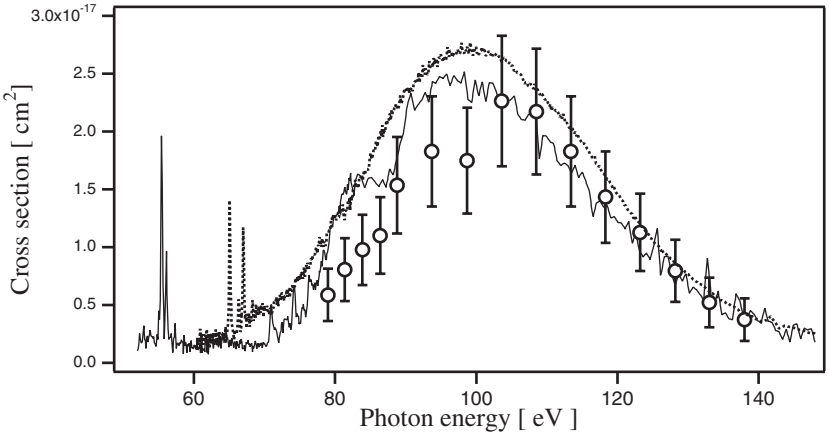

Figure 1. Absolute total photoionization cross section for Xe^+, present measurements (○), previously reported relative cross section [7], normalized at 103.6 eV (——), and absolute total photoionization cross section for Xe [10, 17] (- - - -).

Table 1. Absolute photoionization cross sections determined.

Energy (eV)	$Xe^+ \rightarrow Xe^{2+}$ $\times 10^{-18}$ cm^2	$Xe^+ \rightarrow Xe^{3+}$ $\times 10^{-18}$ cm^2	Sum $\times 10^{-18}$ cm^2
79.0	0.89	5.0	5.9
81.4	1.00	7.1	8.1
83.9	1.10	8.7	9.8
86.4	1.23	9.8	11.0
88.8	1.46	13.9	15.4
93.7	1.27	17.0	18.3
98.7	1.19	16.3	17.5
103.6	1.44	21.2	22.6
108.5	1.23	20.5	21.7
113.4	0.97	17.3	18.3
118.3	0.82	13.5	14.3
123.2	0.67	10.6	11.3
128.2	0.42	7.5	8.0
133.0	0.29	4.9	5.2
138.0	0.29	3.5	3.7

It is well known that almost all the oscillator strength for the 4d electrons in neutral Xe is distributed in the broad giant resonance peak. For example, the oscillator strength distribution between 59.2 and 150.0 eV is reported to be 11.01 [18]; almost all the oscillator strength is consumed in 4d–ϵf transitions.

Sano *et al* [6] and Koizumi *et al* [7] found in the photoionization cross section of Xe^+ ions that there exist many discrete lines which are not seen for the Xe target. They calculated the energy levels using the multiconfiguration Dirac–Fock (MCDF) code and assigned these lines to 4d–*n*p, 4d–*n*f transitions located below 4d ionization thresholds. The 4d–5p transitions at around 55 eV are the most intense transitions among them. As the oscillator strength for 4d electrons is distributed to include these discrete lines, the giant resonance peak is expected to be lowered to some extent in the Xe^+ case. When we integrate over the peak area of the relatively determined cross section corresponding to the 4d–5p transitions, we obtain 1.5×10^{-17} cm^2 eV.

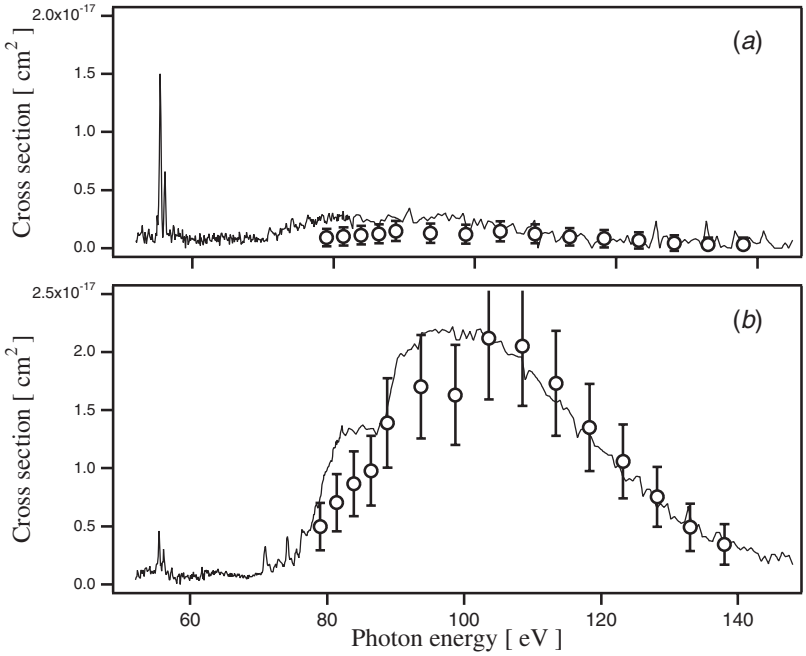

Figure 2. (*a*) Absolute single-photoionization cross sections and (*b*) double-photoionization cross sections for Xe^+. Absolute measurements (○), relative measurements (——). The sum of the relative cross sections was normalized to the absolute total cross section at 103.6 eV.

The photoionization cross section is expressed as $\sigma = 1.098 \times 10^{-16}\ \mathrm{cm}^2\ \mathrm{eV}^{-1}\ \mathrm{d}f/\mathrm{d}\epsilon$, where $\mathrm{d}f/\mathrm{d}\epsilon$ is the oscillator strength per unit energy [19]. Thus, the oscillator strength for these 4d–5p transitions is estimated to be 0.15. Taking into account that there exist many discrete lines, we estimate that only 2–3% of the 4d oscillator strength is used for the discrete transitions. If the rest remains to form the broad giant resonance peak, the cross section should be nearly the same for Xe and Xe^+ targets. Our experimental result provides evidence for the giant resonance peak remaining of the same order of magnitude in Xe^+ as in Xe, taking the experimental error of ±25% into account.

3.2. Single- and double-photoionization cross sections

In figure 2, the single- and double-photoionization cross sections for Xe^+ are shown separately. The energy dependence and the magnitude of single- and double-photoionization cross sections determined absolutely agree well with the relative measurements [6,7] above 100 eV. However, the broad structure seen between 75 and 90 eV in the relative double-photoionization cross section is not so prominent in the present measurement. The same tendency is seen in the single-photoionization cross section below 100 eV, but the absolute cross sections are smaller than the relatively determined cross sections. The present measurement for the Xe^{3+} production cross section shows a significant dip around 99 eV which was not seen in the relative measurements, and the same tendency is reported by Andersen *et al* [12]. This structure is statistically significant because the statistical error of the present measurement is about 5%. The reason for the differences observed between this paper and the relative measurement is not yet clear. It might be due to the different methods of photon intensity determination. In this paper, we used a Si photodiode. We found that the detection efficiency of the Si photodiode changes

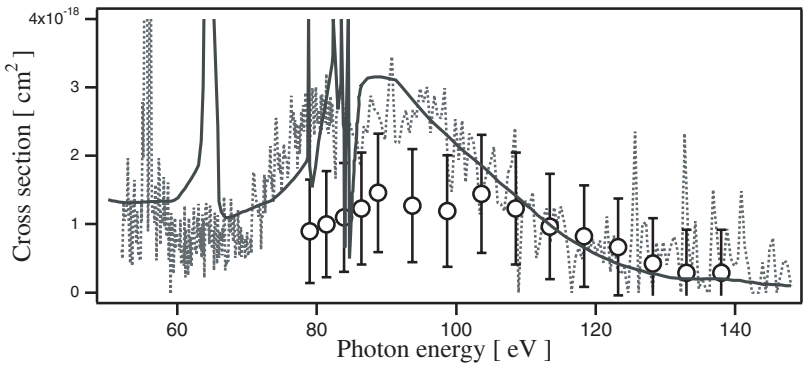

Figure 3. Comparison of the single-photoionization cross sections for Xe^+ obtained experimentally and theoretically. Absolute measurements (○), relative measurements (- - - -), theoretical results reported by Amusia *et al* [20] (——).

strongly around the absorption edge of Si atoms, at around 99.2 and 99.8 eV. Therefore, we carefully avoided using these energies to normalize the relative cross sections. In the relative measurements, a gold-plated photodiode was used and the efficiency was determined by measuring the photoion yield curve of neutral Xe.

Amusia *et al* [20] made a calculation of the single-photoionization cross section for the Xe^+ target using the random phase approximation with exchange (RPAE). Their theoretical results are compared with experimental results in figure 3. They drew attention to the increase of single-photoionization cross section observed at the giant resonance region. They showed that this could not be reproduced in the Hartree–Fock cross section, that is, the sum of direct ionization cross sections of 5s and 5p electrons. They emphasized that the single-photoionization cross section is determined by the interchannel interaction between strong 4d channels with the 5s–ϵp and 5p–ϵd, s transitions.

The agreement between theoretical results and the measured results is excellent in the region higher than 100 eV. The relatively determined cross section also seems to support the theoretical results at the lower energy region, and the theoretical value is about two times larger than the present result at about 90 eV. The calculated value for the single-photoionization cross section for a neutral Xe target reported in that paper was 2.8×10^{-18} cm^2 at 90 eV; this is about 40% larger than the measured value of 2.0×10^{-18} cm^2 [10]. The calculation reported by Amusia *et al* might overestimate the interchannel coupling at the peak energy region of the giant resonance. A large discrepancy is seen for the strong discrete line theoretically obtained at 63.6 eV. Amusia *et al* assigned the line to a 4d–4f transition, but experimentally such a line was not seen. The peak observed at around 55 eV in the relative measurement was assigned to 4d–5p transitions [6, 7]. Therefore, it would be necessary to improve the calculation below the 100 eV region.

4. Summary

The absolute partial and total photoionization cross sections for Xe^+ ions were determined. The structure and energy dependence of the photoionization cross sections of singly charged Xe ions are rather different from those of the neutral Xe atom: however, the absolute cross sections around the giant resonance are nearly the same for both cases. It is concluded that the removal of one outer electron only has a little effect on the magnitude of the total photoionization cross section within the 4d threshold energy region.

Acknowledgments

We would like to thank Professor F Koike for valuable discussions concerning the theoretical interpretation of the spectrum. We are also grateful to Professor A C H Smith for his critical reading of the manuscript, and for his invaluable comments. YI and TK are indebted to Professor T Andersen who organized a fruitful meeting held in the University of Aarhus, in the summer of 2000. The Scandinavia-Japan Sasakawa Foundation supported the meeting. This work was supported in part by a Grant-in-Aid from the JASRI-RIKEN SPring-8 Project, a Grant-in-Aid for Scientific Research on Priority Areas from the Ministry of Education, Science and Culture, and a Grant-in-Aid from the Matsuo Foundation. We gratefully acknowledge this financial support. This experiment was done under approval of the Photon Factory of National Laboratory for High Energy Physics (Proposal no 98G225).

References

[1] Lucatorto T B, McIlrath T J, Sugar J and Younger S M 1981 *Phys. Rev. Lett.* **47** 1124
[2] see, e.g. Charles W C and Lucatorto T B 1987 *Giant Resonances in Atoms, Molecules, and Solids* ed J P Connerade, J M Estava and R C Karnatak (New York: Plenum) pp 137–51
[3] Koizumi T, Itoh Y, Sano M, Kimura M, Kojima T M, Kravis S, Matsumoto A, Oura M, Sekioka T and Awaya Y 1995 *J. Phys. B: At. Mol. Opt. Phys.* **28** 609
[4] D'Arcy R, Costello J T, Kennedy E T, McGuinness C, Mosnier J P and O'Sullivan G 2000 *J. Phys. B: At. Mol. Opt. Phys.* **33** 1383
[5] Kjeldsen H, Andersen P, Folkmann F, Knudsen H, Kristensen B, West J B and Andersen T 2000 *Phys. Rev.* A **62** 020702(R)
[6] Sano M, Itoh Y, Koizumi T, Kojima T M, Kravis S D, Oura M, Sekioka T, Watanabe N, Awaya Y and Koike F 1996 *J. Phys. B: At. Mol. Opt. Phys.* **29** 5305
[7] Koizumi T *et al* 1997 *Phys. Scr.* T **73** 131
[8] Watanabe N *et al* 1998 *J. Phys. B: At. Mol. Opt. Phys.* **31** 4137
[9] Bizau J-M *et al* 2000 *Phys. Rev. Lett.* **84** 435
[10] Becker U, Szostak D, Kerkhoff H G, Kupsch M, Langer B, Wehlitz R, Yagishita A and Hayaishi T 1989 *Phys. Rev.* A **39** 3902
[11] Dolder K 1988 *The Physics of Electronic and Atomic Collisions* ed H B Gilbody, W R Newell, F H Read and A C H Smith (Amsterdam: North-Holland) pp 549–56
[12] Andersen P, Andersen T, Folkmann F, Ivanov V K, Kjeldsen H and West J B 2001 *J. Phys. B: At. Mol. Opt. Phys.* **34** 2009
[13] Lyon I C, Peart B, West J B and Dolder K 1986 *J. Phys. B: At. Mol. Phys.* **19** 4137
[14] http://physics.nist.gov/MajResFac/SURF/Si.detector.html
[15] Shigemasa E, Yan Y and Yagishita A 1995 *KEK Report* No 95-2
[16] Müller A, Achenbach C, Saltzborn E and Becker R 1984 *J. Phys. B: At. Mol. Phys.* **17** 1427
[17] West J B and Morton J 1978 *At. Data Nucl. Data Tables* **22** 103
[18] Berkowitz J 1979 *Photoabsorption, Photoionization, and Photoelectron Spectroscopy* (New York: Academic) p 90
[19] Fano U and Cooper J W 1968 *Rev. Mod. Phys.* **40** 441
[20] Amusia M Ya, Cherepkov N A, Chernysheva L V and Manson S T 2000 *J. Phys. B: At. Mol. Opt. Phys.* **33** L37